J. Fluid Mech. (1970), *vol.* 43, *part* 4, *pp.* 845–859
Printed in Great Britain

Active water-wave absorbers

By JEROME H. MILGRAM
Massachusetts Institute of Technology

(Received 18 August 1969)

The problem considered is that of absorbing two-dimensional water waves in a channel by means of a moving termination at the end of the channel. The problem is formulated for a semi-infinite channel and solutions are determined according to a linearized theory. The motion of the termination that is needed for absorption is determined in the form of a linear operation on the measured surface elevation at a fixed point in the channel so a self-actuating wave-absorbing system can be devised. A theoretical method of studying the stability of such a system is presented. A system of this type was built and experiments with it are described. Wave absorption is demonstrated both for monochromatic waves and for wave pulses. The absorption of a wave pulse is compared with the absorption of the same pulse by a fixed beach making a ten degree angle with the horizontal direction.

1. Introduction

The experimental verification carried out by Ursell, Dean & Yu (1960), of the wave-maker theory of Havelock (1929) suggests the possibility of absorbing two-dimensional waves of small steepness, which are incident on a termination of a channel, by means of a particular motion of this termination. One way to envisage such a situation for the linearized problem is by superposition. If the channel termination were motionless, a wave would be reflected away from the termination when a wave was incident upon it. It is reasonable to expect that a termination motion could be found which would generate a radiated wave that was exactly opposite to the reflected wave. According to the theory of Havelock, the non-radiated component of the fluid motion is negligible at distances more than one-half a wavelength from the termination. If such a situation exists, the channel behaves as though there were complete absorption, except for regions near the termination.

An interesting possibility is to measure some aspect of the fluid motion, determine the termination motion needed for absorption in terms of an operation on the past history of this quantity, and drive the termination such that its motion is a close approximation to this motion. If this can be done, and the entire system is stable, a usable wave absorber would result.

One measurable quantity which seems attractive for operating on, in order to determine the termination motion, is the force exerted on the termination by the fluid. In the experimental work reported here, the termination was a hinged paddle. The incident waves were impinging on one face of the paddle and there

was a short, fluid-filled space between the opposite face and a fixed wall. The fluid motion in this space contributes to the force on the paddle; and since this fluid motion is resonant at certain frequencies, it is not practical to activate the paddle on the basis of measured force. The measured quantity used here is the surface elevation at a point a short distance from the paddle.

2. Theory

2.1. *Formulation of the problem*

The two-dimensional motion of an inviscid, incompressible fluid in a semi-infinite channel is considered. A Cartesian reference frame will be used in which the free surface rest position is at $y = 0$, the bottom of the channel is at $y = -h$ and the rest position of a moving termination of the channel is at $x = 0$. Small amplitude waves are generated at $x = -\infty$. It is assumed that the motion of the channel termination is small in the sense that the deviation from vertical of the slope of any point on the termination is small; and that the horizontal excursion, $\Psi(y,t)$, of any point on the termination from the rest position is small. The fluid motion is assumed to start from an irrotational state so that the fluid velocity can be represented by the gradient of a scalar potential, ϕ, satisfying

$$\nabla^2\Phi = 0, \tag{1}$$

subject to the boundary conditions

$$\Phi_{tt} + g\Phi_y = 0 \quad \text{on} \quad y = 0, \tag{2}$$

$$\Phi_y = 0 \quad \text{on} \quad y = -h, \tag{3}$$

$$\Phi_x = \Psi_t \quad \text{on} \quad x = 0, \tag{4}$$

$$|\nabla\Phi| < \infty \quad \text{at} \quad x = -\infty. \tag{5}$$

Three particular questions must be answered. First, if a sinusoidal wave is generated at $x = -\infty$, and propagates towards the termination, what must $\Psi(y,t)$ be in order that there is no reflected wave? Secondly, can this $\Psi(y,t)$ be determined as a linear functional on the past and present, but not future, values of some measurable quantity of the fluid motion? Thirdly, if the termination motion is given by a prescribed linear functional on a measured quantity of the fluid motion, is the system stable? The remainder of this paper is addressed toward answering these questions.

2.2. *Solution for the fluid motion*

The problem posed by equations (1) to (5) with a time dependence of the form $e^{-i\lambda t}$ is essentially the same as the wave-maker problem solved by Havelock (1929) for real values of λ. This time dependence will be considered here, but λ will be allowed to be complex in order to study the stability of wave-absorbing systems. When λ is complex, the boundary-value problem (1)–(5) is no longer self-adjoint. Solutions to (1) will be determined in the form

$$\Phi(x,y,t) = \phi(x,y)\,e^{-i\lambda t} = \sum_{k=-\infty}^{\infty} C_k\,F_k(x)\,G_k(y)\,e^{-i\lambda t}, \tag{6}$$

where

$$F_k(x) = e^{if_k x} \tag{7}$$

and

$$G_k(y) = \cosh f_k(y+h). \tag{8}$$

The f_k's are the complex solutions for f of

$$fh\tanh fh = \lambda^2 h/g. \tag{9}$$

There are infinitely many solutions for f, being $f_0, f_1, f_2, \ldots$. Let

$$fh = Z = z_r + iz_i. \tag{10}$$

A fundamental region in Z for $Z\tanh Z$ is $0 \leqslant z_i < \frac{1}{2}\pi$, $-\infty < z_r \leqslant \infty$. This strip maps into the entire complex plane. The strip $-\frac{1}{2}\pi < z_i \leqslant 0$, $-\infty \leqslant z_r < \infty$ is also a fundamental region as are the strips $(n-\frac{1}{2})\pi \leqslant z_i < (n+\frac{1}{2})\pi$, $-\infty < z_r \leqslant \infty$, for any positive integer n, and the strips $(n-\frac{1}{2})\pi < z_i < (n+\frac{1}{2})\pi$, $-\infty \leqslant z_r < \infty$ for any negative integer n. Equation (9) has a solution on each strip. Since (9) is even in f, if f_k is a solution, $-f_k$ is also a solution. The boundary condition of boundedness at $x = -\infty$, (5), is satisfied only by eigenfunctions, $F_k(x)\,G_k(y)$, for which $\operatorname{Im} f_k \geqslant 0$. Therefore there is one eigenvalue f_k and one associated eigenfunction on each strip above the real axis of the Z plane. The only strip below the real axis that can contain an eigenvalue and associated eigenfunction is the strip below and adjacent to the real axis, and this is permitted only if this eigenvalue is real. Thus $\phi(x, y)$ can be expressed as

$$\phi(x,y) = A_0' \cosh f_0(y+h)\, e^{-if_0 x} + \sum_{n=0}^{\infty} A_n \cosh f_n(y+h)\, e^{if_n x}. \tag{11}$$

Here, f_0 is on the strip adjacent to and above the real axis of the Z plane and f_n is on the strip $(n-\frac{1}{2})\pi \leqslant z_i < (n+\frac{1}{2})\pi$. If $\operatorname{Im} f_0 \neq 0$, $A_0' = 0$.

Suppose the motion of the channel termination is given by

$$\Psi(y,t) = B\psi(y)\, e^{-i\lambda t}, \tag{12}$$

where $\psi(y)$ is a known, real function determined by the mechanics of the termination and B is a complex constant. The boundary condition at the termination, (4), requires that

$$(A_0 - A_0')\cosh f_0(y+h) + \sum_{n=1}^{\infty} A_n f_n \cosh f_n(y+h) = -B\lambda\psi(y). \tag{13}$$

If λ is complex, the f's are complex and since the boundary-value problem is not self-adjoint, the eigenfunctions $G_k(y)$ are not orthogonal.

$$\int_{-h}^{0} G_k(y)\, G_n^*(y)\, dy \neq 0 \tag{14}$$

for all k when $n \neq k$, if λ is complex.

However, the G_k's do satisfy

$$\int_{-h}^{0} G_k(y)\, G_n(y)\, dy = 0 \quad \text{for} \quad k \neq n. \tag{15}$$

Therefore,

$$\left.\begin{array}{ll} \text{for} & n = 0, \quad A_0 - A_0' \\ \text{for} & n \neq 0, \quad A_n \end{array}\right\} = -\frac{\lambda}{f_n} B \frac{I_n^{(2)}}{I_n^{(1)}}, \tag{16}$$

where

$$I_n^{(2)} = \int_{-h}^{0} \psi(y)\cosh f_n(y+h)\, dy \tag{17}$$

and

$$I_n^{(1)} = \tfrac{1}{2}h\left[1 + \frac{1}{2f_n h}\sinh 2f_n h\right]. \tag{18}$$

As an example, the problem of determining the fluid motion is solved here for the case where the termination is a paddle hinged at $y = -p$, with a solid wall between the pivot position and the bottom of the channel. For this termination,

$$\psi(y) = \begin{cases} y+p, & y \geqslant -p, \\ 0, & y < -p, \end{cases} \tag{19}$$

and

$$I_n^{(2)} = \frac{p}{f_n}\sinh f_n h + \frac{1}{f_n^2}[\cosh f_n(h-p) - \cosh f_n h]. \tag{20}$$

The paddle angle, θ, is given by

$$\theta = B e^{-i\lambda t}. \tag{21}$$

Equation (16) does not uniquely specify A_0 or A_0', but gives their difference. If λ is complex, boundedness of the fluid motion at $x = -\infty$, (5), requires that $A_0' = 0$. If λ is real, identical solutions for the fluid motion are obtained if λ is replaced by $-\lambda$. To be definite, if λ is real, take $\lambda > 0$. Similar remarks apply to f_0 which is real if λ is real, so take $f_0 > 0$ if λ is real. Then A_0 is the coefficient of the positive-going wave generated at $x = -\infty$. For a known value of A_0, (16) determines A_0'.

If sinusoidal waves are generated at $x = -\infty$ with a velocity potential of amplitude A_0, A_0' is the amplitude of the velocity potential of the reflected wave. For complete absorption, $A_0' = 0$, in which case (16) requires that

$$B = -A_0 \frac{f_0 I_0^{(1)}}{\lambda I_0^{(2)}}. \tag{22}$$

For complete absorption with the hinged paddle termination,

$$B = -\frac{f_0^2}{4\lambda} A_0 \frac{2f_0 h + \sinh f_0 h}{p f_0 \sinh f_0 h + \cosh f_0(h-p) - \cosh f_0 h}. \tag{23}$$

The surface elevation, $N(x,t)$, can be obtained from the velocity potential by use of the kinematic free surface condition,

$$\Phi_y = N_t \quad \text{at} \quad y = 0. \tag{24}$$

Expressing N in the form

$$N(x,t) = \eta(x)\, e^{-i\lambda t} \tag{25}$$

and using (25) gives

$$\eta(x) = -\frac{f_0}{i\lambda}\sinh f_0 h (A_0 e^{if_0 x} + A_0' e^{-if_0 x}) - \frac{1}{i\lambda}\sum_{n=1}^{\infty} f_n A_n \sinh f_n h\, e^{if_n x}. \tag{26}$$

The problem at hand is to determine the termination motion as a linear operation on the past history of the surface elevation at a point, say at $x = -d$. The frequency dependent ratio of the complex amplitude of the termination motion, B, to the complex amplitude of the surface elevation at $x = -d$, $\eta(-d)$, for no reflected wave is called $H_a(\lambda)$ and is given by

$$H_a(\lambda) = i \Big/ \sum_{n=0}^{\infty} \frac{I_2^{(n)}}{I_1^{(n)}} e^{-if_n d} \sinh f_n h. \tag{27}$$

Let $h_a(t)$ be the inverse Fourier transform of $H_a(\lambda)$.

$$h_a(t) = \frac{1}{2\pi}\int_{-\infty}^{\infty} H_a(\lambda)\, e^{i\lambda t}\, d\lambda, \tag{28}$$

where $H_a(\lambda)$ for negative λ is defined by $H_a(\lambda) = H_a^*(-\lambda)$. The time-dependent amplitude of the termination motion $b(t)$ for no reflected wave is then given by the convolution of the surface elevation at $x = -d$, $N(-d, t)$, and $h_a(t)$.

$$b(t) = \int_{-\infty}^{\infty} N(-d, t-\tau)\, h_a(\tau)\, d\tau. \tag{29}$$

If $h(t) = 0$ for $t < 0$, then $b(t)$ depends only on the past values of $N(-d, t)$. It is reasonable that $h(t)$ equals zero for $t < 0$ as this would be implied by a criterion that the termination be motionless before any incident wave front reached it.

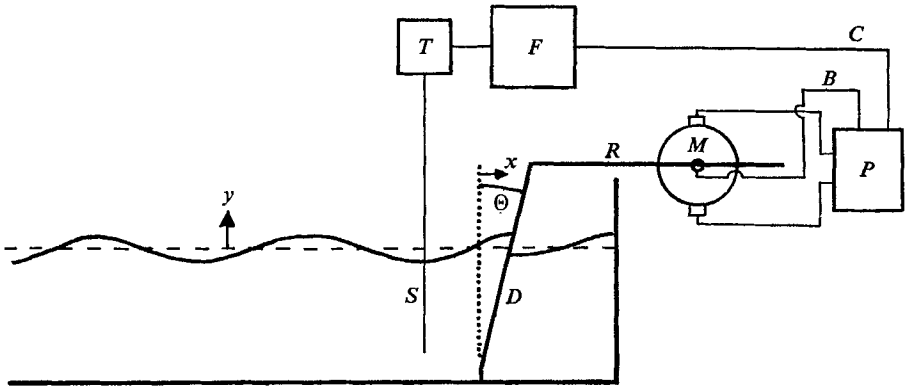

FIGURE 1. The wave-absorbing termination. – – –, Rest position of the free surface ($y = 0$); ....., rest position of the absorbing termination ($x = 0$); S, surface elevation sensing probe; T, surface elevation to voltage transducer; F, active electric filter; C, position control actuating signal; P, electric components of the position control servo-mechanism; M, position control servo-motor; R, paddle drive rod; D, paddle; B, position feedback signal; Θ, paddle angle.

However, a proof that $h(t) = 0$ for $t < 0$ requires demonstrating that $H_a(\lambda)$ is analytic everywhere in $\mathrm{Im}\,\lambda > 0$. Rather than attempt to carry out this demonstration, the experiments are appealed to, where $H_a(\lambda)$ is approximated by a function that is analytic in $\mathrm{Im}\,\lambda > 0$ and waves are absorbed by the resulting system. Equation (29) holds for any incident wave time dependence, not only $e^{-i\lambda t}$.

2.3. *Stability of wave-absorbing systems*

It is assumed here that a linear electro-mechanical device, taking the surface elevation at $x = -d$ as input and providing the amplitude of the termination motion as output, has a complex ratio of input to output amplitudes given by $H_e(\lambda)$. The method of synthesizing $H_e(\lambda)$ in a realizable form is described in the appendix.

A wave-absorbing system, activated by the surface elevation at $x = -d$ is shown in figure 1. For such a system to be usable, it must be stable. An unstable system is taken to mean a system for which a small disturbance generated by the termination grows ceaselessly with increasing time. Since motions having the time dependence $e^{-i\lambda t}$ are considered, the system is unstable if there are any normal modes for which $\mathrm{Im}\,\lambda > 0$.

The hydrodynamics of the problem specifies a relationship between the complex amplitudes of the termination motion, B, and the surface elevation at $x = -d$. The ratio of these complex amplitudes is called $H_h(\lambda)$. To avoid ambiguity, take $\mathrm{Re} f_0 > 0$ which can be done arbitrarily because if f_0 is an eigenvalue, $-f_0$ is also an eigenvalue. Then A_0 is the coefficient of a wave travelling towards the termination which is taken to be zero when normal modes of the system are being determined

Using (16), (21) and (26) yields

$$H_h(\lambda) = \frac{B}{[\eta]_{x=-d}} = i \Big/ \left[\frac{I_0^{(2)}}{I_0^{(1)}} \sinh f_0 h \frac{A_0 e^{-if_0 d} + A_0' e^{if_0 d}}{A_0 - A_0'} + \sum_{n=1}^{\infty} \frac{I_n^{(2)}}{I_n^{(1)}} \sinh f_n h \, e^{-if_n d} \right]. \tag{30}$$

However, the termination driving system requires that

$$\frac{B}{[\eta]_{x=-d}} = H_e(\lambda). \tag{31}$$

Equations (30) and (31) can be satisfied simultaneously if and only if

$$H_e(\lambda) = H_h(\lambda). \tag{32}$$

This is the characteristic equation of the system. Any values of λ for which (32) holds when $A_0 = 0$ are natural frequencies of the system. If, for any of these values of λ, $\mathrm{Im}(\lambda) > 0$, the system will be unstable at that frequency. If (32) holds for real values of λ, the system will be neutrally stable at that frequency.

One way to find any values of λ for which (32) holds is to search the complex λ plane point by point to find which points, if any, give a solution to (32). Since this is very tedious, a method essentially the same as that used by Nyquist (1932) is recommended instead.

Let
$$q(\lambda) = 1 - \frac{H_e(\lambda)}{[H_h(\lambda)]_{A_0=0}}. \tag{33}$$

The zeros of $q(\lambda)$ give the natural frequencies of the system. It is assumed that $H_e(\lambda)$ has no poles in the upper half of the λ plane (see appendix).

It is further assumed that

$$\lim_{\lambda \to \infty} \left| \frac{H_e(\lambda)}{H_h(\lambda)} \right| < 1. \tag{34}$$

This is a good design criterion to use in order to minimize the effects of high frequency noise. $H_h(\lambda)$ has no zeros on any finite part of the λ plane, which along with the above assumptions about $H_e(\lambda)$ implies that $q(\lambda)$ has no poles on the upper half of the λ plane.

Consider the closed contour comprised of the real axis and the upper infinite semi-circle in the λ plane. From the theorem of the principle of argument, the number of zeros of $q(\lambda)$ inside a closed contour containing no poles of $q(\lambda)$ is equal to $1/2\pi$ times the change in the argument of $q(\lambda)$ observed when traversing the closed contour once in the positive sense. Now consider the contour in the complex q plane onto which the closed contour in the λ plane maps. The number of times this contour encircles the origin of the q plane equals the number of

zeros of $q(\lambda)$ in the upper half of the λ plane. The mapping of the upper semi-circle of the q plane does not encircle the origin of the q plane since on this semi-circle, $\mathrm{Re}\, q(\lambda) > 0$. Therefore, if the mapping of the real axis of the λ plane does not encircle the origin of the q plane, the system is stable. Hence the stability of the system can be assessed by examining the values of $q(\lambda)$ only on the real axis of the λ plane.

2.4. *The reflexion coefficient of a wave-absorbing system*

Since $H_e(\lambda)$ is not exactly equal to $H_a(\lambda)$ in general, an active wave absorber will not necessarily absorb waves completely. To determine the reflexion coefficient, (32) is applied for the case when $A_0 \neq 0$. The reflexion coefficient is then given by $|A_0'/A_0|$ which will be called $\epsilon(\lambda)$.

$$\epsilon(\lambda) = \left| \frac{i - H_e(\lambda) \sum_{n=0}^{\infty} (I_n^{(2)}/I_n^{(1)}) \sinh f_n h \, e^{-if_n d}}{i + H_e(\lambda) \left[(I_0^{(2)}/I_0^{(1)}) \sinh f_0 h \, e^{-if_0 d} - \sum_{n=1}^{\infty} (I_n^{(2)}/I_n^{(1)}) \sinh f_n h \, e^{if_n d} \right]} \right|. \tag{35}$$

3. The design of a wave-absorbing system for a hinged paddle absorber

In this section the design of a function, $H_e(\lambda)$, is carried out for the absorber used in the experiments. The absorbing termination used is of the hinged paddle type as described in the example of § 2.2. The physical parameters for the channel used in the experiments are:

$$g = 980{\cdot}6 \text{ cm/sec}^2, \tag{36}$$

$$h = 12{\cdot}70 \text{ cm}, \tag{37}$$

$$p = 11{\cdot}42 \text{ cm}, \tag{38}$$

$$d = 5{\cdot}08 \text{ cm}. \tag{39}$$

The frequency range over which wave absorption is desired is from three to thirteen radians per second. $H_e(\lambda)$ must closely approximate $H_a(\lambda)$ over this range. Using (18) and (20), $H_a(\lambda)$ is given by (27). $H_a(\lambda)$ is shown for λ between three and thirteen radians per second in figure 2. Observation of this figure shows that $H_e(\lambda)$ should behave roughly like $-i/\lambda$. However, one design constraint is that $H_e(\lambda)$ have a zero at $\lambda = 0$ to prevent drift. Therefore, let

$$H_e(\lambda) = -\frac{\lambda}{(\lambda - a)^2} H_e^t(\lambda), \tag{40}$$

where a is a negative imaginary number having a magnitude considerably less than the lowest radian frequency at which wave absorption is desired. a is arbitrarily chosen to be $-0{\cdot}4i$. For complete absorption,

$$H_e^t(\lambda) = -\frac{(\lambda + 0{\cdot}4i)^2}{\lambda} H_a(\lambda). \tag{41}$$

$[-(\lambda+0{\cdot}4i)^2/\lambda]\,H_a(\lambda)$ is shown in figure 2. This indicates that $H_e^t(\lambda)$ should have more poles than zeros. Choosing a function having one zero and two poles on the imaginary axis of the λ plane to approximate $H_e^t(\lambda)$ and optimizing their location to minimize the mean square error as described in the appendix gives the following function, $H_e^d(\lambda)$, for a design of $H_e(\lambda)$:

$$H_e^d(\lambda) = 930{\cdot}3i\,\frac{\lambda(\lambda+10{\cdot}70i)}{(\lambda+0{\cdot}4i)^2\,(\lambda+49{\cdot}97i)\,(\lambda+82{\cdot}29i)}. \tag{42}$$

To determine whether or not a wave-absorbing system having a filter-system function $H_e^d(\lambda)$ as given above is stable, the mapping given by (33) of the real axis of the λ plane in the q plane is shown in figure 3. Since the arc does not encircle the origin of the q plane, the system is stable according to § 2.3.

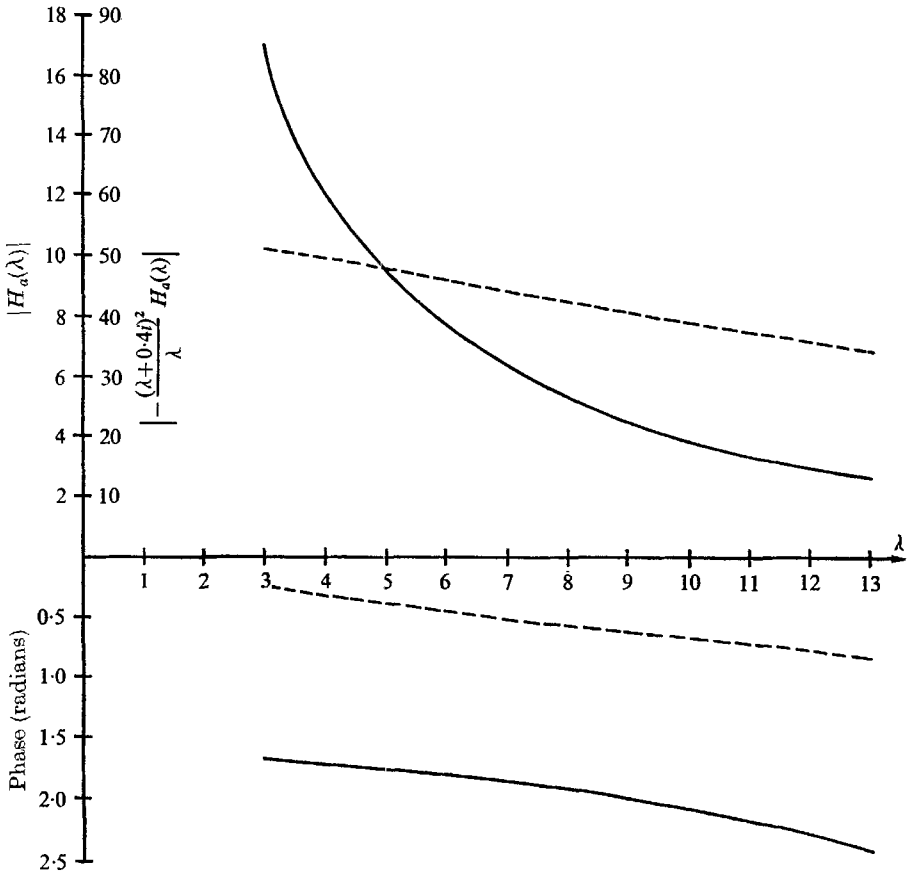

FIGURE 2. ——, $H_a(\lambda)$ and – – –, $[-(\lambda+0{\cdot}4i)^2/\lambda]\,H_a(\lambda)$ for real values of λ.

4. Experiments

4.1. *Experimental apparatus*

An aluminium wave channel was built, having a length of 335 cm, a depth of 19·1 cm and a width of 30·5 cm. The side walls were kept plane and parallel to a tolerance of 0·02 cm by means of adjustable brackets on each side wall, outside

the channel, spaced 30·5 cm apart, except near paddles fitted at each end of the tank where the brackets were more closely spaced. The aluminium paddles were 0·635 cm thick and had their pivots 1·27 cm above the bottom of the channel. There were solid plates between the pivots and the channel bottom. The distance between the inside faces of the paddles was 305 cm when both paddles were vertical. The channel was filled with water to a depth of 12·7 cm.

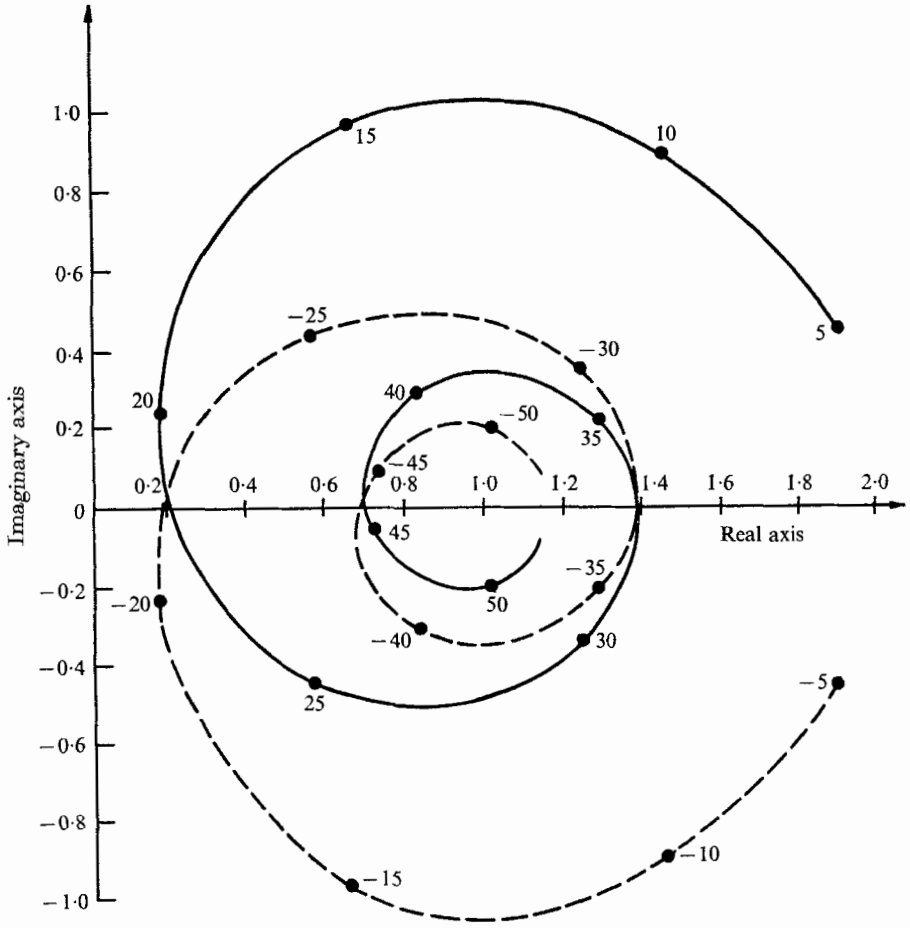

FIGURE 3. $q(\lambda)$ for real values of λ from the example in (3) and (4). The contour shown is the mapping of the real axis of the λ plane given by (34) ($\omega = \mathrm{Re}\,\lambda$). Numbers at the points are the values of ω in radians/sec.

An adjustable speed motor was attached to one of the paddles through an adjustable bell crank mechanism for purposes of making waves of adjustable height and frequency. A capacitance-type surface elevation transducer with a 0·159 cm diameter probe was attached to a motor driven carriage to be able to scan the surface elevation at different positions. The capacitance probe was vibrated vertically at 120 Hz to avoid errors due to variations in the meniscus. The 120 Hz signal added to the surface elevation signal was filtered out. This transducer gave an output proportional to the surface elevation (Milgram 1965).

The wave-absorbing apparatus is shown schematically in figure 1. A second surface elevation transducer was installed with its probe 5·08 cm from the vertical rest position of the paddle. The output voltage from this transducer served as input to an active electric filter having a system function $H_e^m(\lambda)$. The output voltage from the filter was used to activate a position control servo-mechanism. The wave-absorbing paddle was driven by the servo-motor through a rack and pinion drive.

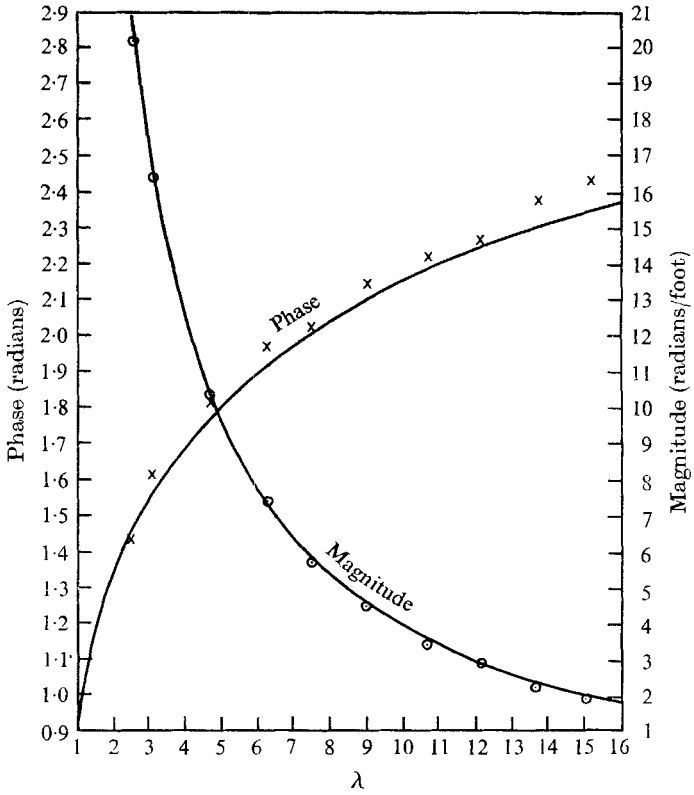

FIGURE 4. The designed system function, $H_e^d(\lambda)$, and the measured system function, $H_e^m(\lambda)$, for real values of λ. ——, $H_e^d(\lambda)$; ⊙, $|H_e^m(\lambda)|$; ×, arg $[H_e^m(\lambda)]$.

An active electric filter was built to have the system function $H_e^d(\lambda)$ as given by (42). Since small errors in the parameters of the circuit elements and errors in the position control servo-mechanism affect the filter response, the actual system function, $H_e^m(\lambda)$, was measured for real values of λ. This was done by disconnecting the surface elevation signal from the input of the filter and using an externally generated sinusoidal signal as input. The position control feed-back signal came from a potentiometer geared to the paddle drive rack gear. The voltage output from this potentiometer was used as the output signal in determining the system function. $H_e^d(\lambda)$ and $H_e^m(\lambda)$ are shown in figure 4 for real values of λ.

4.2. *Determination of the reflexion coefficient*

When a wave channel is operating sinusoidally, the surface elevation at points more than one wavelength from the channel terminations can be represented by

$$N(x,t) = \operatorname{Re}\eta(x)\,e^{-i\omega t} \tag{43}$$

where

$$\eta(x) = a[e^{i\alpha_0 x} + \epsilon\, e^{(-i\alpha_0 x + i\delta)}] \tag{44}$$

ϵ is the reflexion coefficient and δ is a phase angle. Solving for ϵ gives

$$\epsilon = \frac{|\eta|_{\max} - |\eta|_{\min}}{|\eta|_{\max} + |\eta|_{\max}}. \tag{45}$$

Values for $|\eta|_{\max}$ and $|\eta|_{\min}$ were found by attaching the output signal of the carriage-mounted wave-height transducer to a paper chart recorder and driving the carriage very slowly along the channel.

4.3. *Measurements*

When experiments with the wave absorber in operation were carried out, the motion of the absorbing paddle was sinusoidal for wave frequencies below eight radians per second. At higher incident wave frequencies, the absorber motion

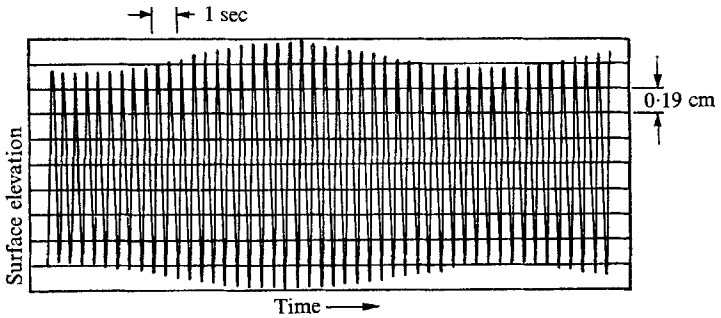

FIGURE 5. A sample chart record for determining the reflexion coefficient. The quantity shown is the surface elevation *vs.* time as measured by a wave height transducer that moves slowly along the longitudinal axis of the wave channel. For this record, the ratio of mean wave height to wavelength is 0·05 and the wave frequency is 2·07 Hz. The reflexion coefficient as given by (45) is 0·113.

was sinusoidal shortly after motion began, but later quite a lot of second harmonic motion was observed. In order to measure just the fundamental frequency at the moving wave-height transducer, the output signal from this transducer was passed through an adjustable low pass filter, set so the second harmonic was attenuated ten times as much as the fundamental.

Reflexion coefficients were then measured for frequencies between three and thirteen radians per second for various wave-maker strokes. This was done with the moving wave height transducer connected to a chart recorder and using (45). A typical chart record is shown in figure 5. Figure 6 shows the theoretical reflexion coefficients for $H_e(\lambda)$ equal to $H_e^m(\lambda)$ and $H_e^d(\lambda)$ as well as the measured reflexion coefficients.

It can be shown that if a wave pulse is incident on a wave absorber having a certain frequency band for wave absorption, that part of the pulse which is in the absorption band will be absorbed (see e.g. Milgram 1965). Experiments were carried out for a pulse wave generated by letting the wave-making paddle move through one half of a sinusoidal cycle. The surface elevation was measured as

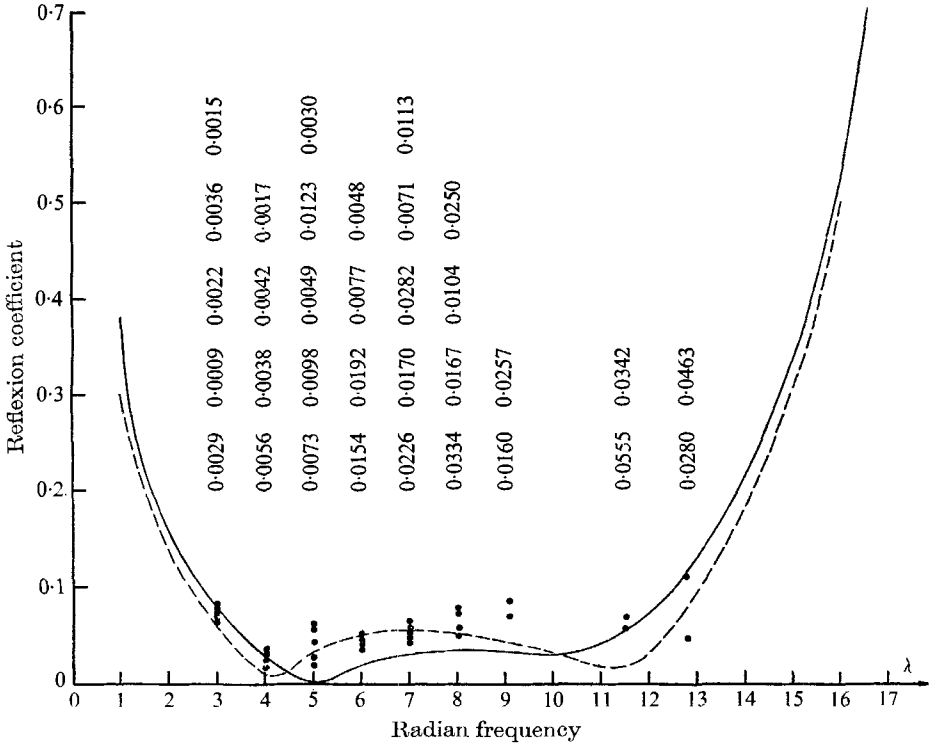

FIGURE 6. Reflexion coefficients. —, theory for $H_e(\lambda) = H_e^d(\lambda)$; ––, theory for $H_e(\lambda) = H_e^m(\lambda)$; ●, experimental measurement. The numbers refer to the ratio of wave height (trough to crest) to wavelength for the points beneath them.

a function of time at a fixed point near the centre of the channel. This record as well as the record of absorbing paddle angle *versus* time are shown in figure 7.

For purposes of comparison, similar records of the surface elevation were made with the absorber replaced by a ten degree sloping beach and by a rigid vertical wall. These records are shown in figures 8 and 9.

4.4. *Interpretation of experimental results*

The difference between the measured reflexion coefficient and that predicted by (35) for an absorbing system function $H_e^m(\lambda)$ is less than 0·02 for most experimental points. The major exception to this occurs for a wave radian frequency of 9·25 radians/sec. Quite a lot of second harmonic motion was observed at this frequency and if the combined first and second harmonic amplitude resulted in non-linear effects in the servo-mechanism, such as limiting or overloading, errors

in the fundamental frequency motion would occur. Calculations indicate a reflexion coefficient of 1·8 at a radian frequency of 18·5 radians/sec. Depending on the phase of the reflected wave, the finite length channel may or may not be

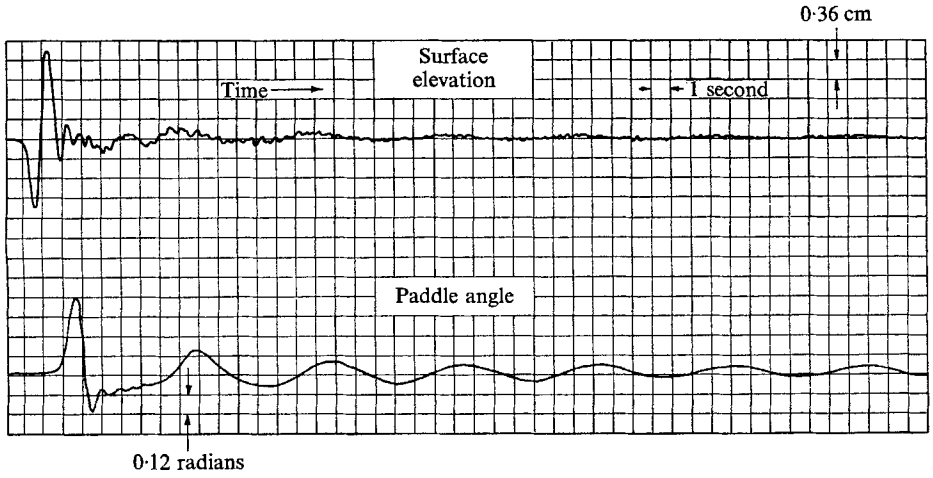

FIGURE 7. The surface elevation near the centre of the channel and the paddle angle records for a pulse wave generated at one end of the channel and the active wave absorber at the other end.

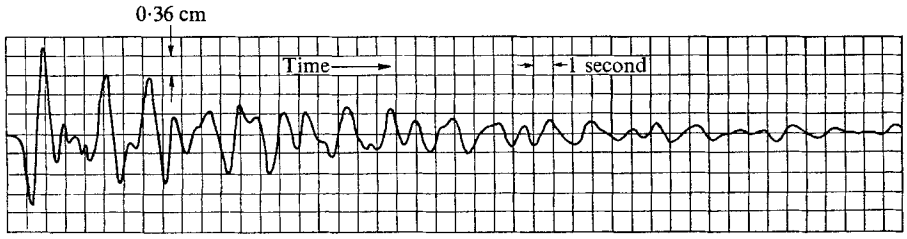

FIGURE 8. The surface elevation for the pulse of figure 7 with the wave absorber replaced by a 10° sloping beach.

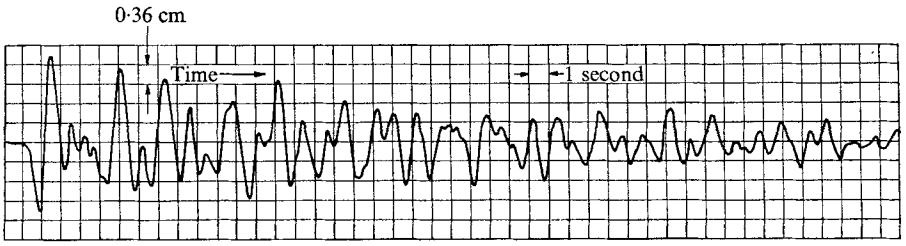

FIGURE 9. The surface elevation for the pulse of figure 7 with the wave absorber replaced by a rigid wall.

unstable with respect to standing waves at all frequencies for which the reflexion coefficient lies between 1·0 and 2·0. The channel should be unstable with respect to standing waves at all frequencies for which the reflexion coefficient exceeds 2·0, which occurs for frequencies between 19 and 23·5 radians per second when

$H_e(\lambda)$ equals $H_e^d(\lambda)$. The reason why this instability was not directly observed is attributed to the fact that the position control servo-mechanism cannot properly follow the higher frequencies.

The experiments with the pulse wave clearly indicate absorption over the designed frequency bandwidth. Significant reflexion was found at frequencies above and below this range. The reason why so little absorption resulted from the 10 degree sloping beach is that the wave was of small steepness and the sloping beach uses non-linear effects to cause wave breaking.

5. Conclusions

The theoretical and experimental results given here indicate that it is possible to move a channel termination in a manner such that an incident wave will be absorbed. This is certainly expected due to the validity of superposition of small waves and the wave-maker theory of Havelock (1929).

A new conclusion that the termination motion needed to absorb waves can be obtained by a linear operation on a measured quantity of the fluid motion. This allows the construction of a self-actuating, active absorbing termination.

In the synthesis of a wave-absorbing system function, three criteria were used in addition to the requirement that the synthesized function be a close approximation to the ideal absorbing system function for the range of wave frequencies to be absorbed. These additional criteria are that: (i) the complete system be stable, (ii) the absorbing system have zero response at a frequency of zero to prevent drift, and (iii) the absorbing system function $H_e^d(\lambda)$ have an amplitude less than the hydrodynamic system function $H_a(\lambda)$ for high frequencies to prevent high frequency noise. From the experiments it is clear that a fourth criterion should be added; namely that the reflexion coefficient be less than 1·0 for all λ. This would prevent high frequency amplification from causing significant second harmonic effects.

The error between theory and experiment shown in figure 6 shows no definite trend. Some measured values of reflexion coefficient are larger than theoretically predicted and some are smaller. Similar scatter exists in the error as a function of wave amplitude; and therefore finite-amplitude effects were not important in affecting the reflexion coefficient of the first-order waves in the experiments.

The ratios of wave height (peak to trough) to wavelength used in the experiments varied between 0·0009 and 0·0555. More second harmonic motion was observed for higher values of this ratio than for smaller values. The second harmonic was especially apparent when the reflexion coefficient at a frequency equal to that of the second harmonic was large. The initial generation of second (and higher) harmonic effects is due to non-linearities in the servo-mechanism and to non-linearities in the fluid motion. The servo-mechanism non-linearities result from requiring too much instantaneous power and could easily be overcome with a larger servo-mechanism. To deal with the non-linearities in the fluid mechanics higher order theories must be carried out. This has been done up to second order (Milgram 1965), but it is complicated both mathematically and from the standpoint of implementation.

Waves of small steepness are difficult to absorb with conventional sloping beaches and easier to absorb with an active wave absorber. The converse applies to large waves so the absorption methods are complementary. The agreement between theory and experiment for the linear wave absorber is sufficiently good to provide experimental confirmation of the theory.

Appendix. Synthesis of wave-absorbing system functions

It is assumed that a surface elevation transducer provides electric voltage equal to the surface elevation at $x = -d$. This voltage serves as input to an electric filter having the system function $H_e(\lambda)$ and the output voltage from the filter actuates a position control servo-mechanism that drives the movable termination of the channel (figure 1). If $H_e(\lambda)$ equals $H_a(\lambda)$ over a specified frequency range, waves in this frequency range will be absorbed. The problem here is to closely approximate $H_a(\lambda)$ by $H_e(\lambda)$ over the specified frequency range. In order that $H_e(\lambda)$ can be synthesized from lumped parameter circuit elements it will be sought in the following form:

$$H_e(\lambda) = iC_e \frac{(\lambda-a)(\lambda-b)\dots}{(\lambda-q)(\lambda-r)(\lambda-s)\dots}, \tag{A 1}$$

where C_e is a real constant. One criterion that will be used here is that the filter be stable, without the effects of the hydrodynamic feed-back. This criterion may not be necessary, but it is good design practice. This requires that no poles of $H_e(\lambda)$ lie in the upper half of the λ plane. To ensure that $H_e(\lambda)$ does not have any neutrally stable frequencies, poles will be excluded from the real axis also. In order that the filter be realizable, all poles and zeros at which $\mathrm{Re}\,\lambda \neq 0$ must occur in pairs symmetrically located with respect to the imaginary axis of the λ plane.

A computer program has been prepared which determines $H_e(\lambda)$ in the form (A 1) so that the mean square error between $H_a(\lambda)$ and $H_e(\lambda)$ is minimized over a prescribed frequency range. The program requires a set of positions of the poles and zeros as input and it relocates the poles and zeros so as to minimize the mean square error. The program automatically adds a zero at $\lambda = 0$ so the system will not drift. In designing filters, it is advised that the number of poles exceed the number of zeros so that high frequency noise is attenuated.

REFERENCES

HAVELOCK, T. H. 1929 Forced surface waves on water. *Phil. Mag.* **8**, 569–576.

MILGRAM, J. H. 1965 Compliant water-wave absorbers. *M.I.T. Department of Naval Architecture and Marine Engineering Report* no. 65-13.

NYQUIST, H. 1932 Regeneration theory. *Bell Syst. Tech. J.* **11**, 126–147.

URSELL, F., DEAN, R. & YU, Y. 1960 Forced small amplitude water waves; a comparison of theory and experiment. *J. Fluid Mech.* **7**, 33–52.